1-1-2001

Possible roles of protein kinase A in cell motility and excystation of the early diverging eukaryote Giardia lamblia

Erika S. Abel
University of Central Florida

Barbara J. Davids

Liza D. Robles
University of Central Florida

Clarence E. Loflin
University of Central Florida

Frances D. Gillin

Recommended Citation

Abel, Erika S.; Davids, Barbara J.; Robles, Liza D.; Loflin, Clarence E.; Gillin, Frances D.; and Chakrabarti, Ratna, "Possible roles of protein kinase A in cell motility and excystation of the early diverging eukaryote Giardia lamblia" (2001). *Faculty Bibliography 2000s*. 2890.
https://stars.library.ucf.edu/facultybib2000/2890

Authors

Erika S. Abel, Barbara J. Davids, Liza D. Robles, Clarence E. Loflin, Frances D. Gillin, and Ratna Chakrabarti

Possible Roles of Protein Kinase A in Cell Motility and Excystation of the Early Diverging Eukaryote *Giardia lamblia**

Erika S. Abel‡, Barbara J. Davids§, Liza D. Robles‡, Clarence E. Loflin‡, Frances D. Gillin§, and Ratna Chakrabarti‡¶

From the ‡Department of Molecular Biology and Microbiology, University of Central Florida, Orlando, Florida 32826 and the §Department of Pathology, Division of Infectious Diseases, University of California, School of Medicine, San Diego, California 92103

Since little is known of how the primitive protozoan parasite, *Giardia lamblia*, senses and responds to its changing environment, we characterized a giardial protein kinase A (gPKA) catalytic subunit with unusual subcellular localization. Sequence analysis of the 1080-base pair open reading frame shows 48% amino acid identity with the cyclic AMP-dependent kinase from *Euglena gracilis*. Northern analysis indicated a 1.28-kilobase pair transcript at relatively constant concentrations during growth and encystation. gPKA is autophosphorylated, although amino acid residues corresponding to Thr-197 and Ser-338 of human protein kinase A (PKA) that are important for autophosphorylation are absent. Kinetic analysis of the recombinant PKA showed that ATP and magnesium are preferred over GTP and manganese. Kinase activity of the native PKA has also been detected in crude extracts using kemptide as a substrate. A myristoylated PKA inhibitor, amide 14-22, inhibited excystation with an IC$_{50}$ of 3 μM, suggesting an important role of gPKA during differentiation from the dormant cyst form into the active trophozoite. gPKA localizes independently of cell density to the eight flagellar basal bodies between the two nuclei together with centrin, a basal body/centrosome-specific protein. However, localization of gPKA to marginal plates along the intracellular portions of the anterior and caudal pairs of flagella was evident only at low cell density and higher endogenous cAMP concentrations or after refeeding with fresh medium. These data suggest an important role of PKA in trophozoite motility during vegetative growth and the cellular activation of excystation.

Infection with *Giardia lamblia* is a major global cause of water-borne diarrheal disease (1). Nonetheless, neither its basic biology nor the pathophysiology of infection is well understood. To date, no giardial toxin or conventional virulence factor has been identified by biological (2) or genomic studies (3). Therefore, it is critical to understand how the parasite survives in the external environment and infects and colonizes a new host. *G. lamblia* has two life cycle stages that are each remarkably well adapted to survival in very different and inhospitable environments. The dormant, quadrinucleate cyst persists for months in fresh cold water (4). Infection is initiated by ingestion of cysts (5). Exposure of cysts to gastric acid during passage through the host stomach triggers the rapid and dramatic differentiation known as excystation. After entry into the small intestine and stimulation by specific factors (6), the parasite emerges and divides into two equivalent binucleate trophozoites that attach to and colonize the human small intestine. The cyst wall must remain intact during passage through the stomach acid; however, once the cyst enters the small intestine, the wall must open rapidly to enable the parasite to emerge and attach to host enterocytes.

In the small intestine, giardial trophozoites are exposed to complex and everchanging concentrations of hydrogen ions and nutrients, as well as bile acids and digestive enzymes (7). As enterocytes migrate to the tip of the villus, where they are sloughed off into the lumen, attached trophozoites must be able to sense and respond rapidly to environmental signals to remain in the small intestine. Since excystation entails such rapid responses to environmental stimuli, we hypothesized that protein kinase-mediated signaling might be very important. Thus, cell-signaling pathways may be crucial to both giardial colonization in the small intestine and to the cellular activation of excystation. Although many protein kinase gene fragments have been identified by large scale genomic sequencing (Ref. 8; see also the web site for the *Giardia* Genome Project Database (Marine Biological Laboratory, Woods Hole, MA)), there is little understanding of their potential roles in giardial survival and growth in the small intestine or in regulation of differentiation.

In many eukaryotic cells, cyclic AMP (cAMP)-dependent signaling pathways play a critical role in regulating cell growth, metabolism, and differentiation (10, 11). Protein kinase A (PKA,[1] EC 2.7.1.37), the defining enzyme of the cyclic AMP-dependent signaling pathway alters protein activity by phosphorylation at serine/threonine residues within the motif RRX(S/T) (12). PKA is one of the simplest protein kinases known because of its dissociative mechanism of activation (13). PKA holoenzyme, a catalytically inactive form, is a tetrameric complex containing two identical catalytic (C) subunits bound to a homodimer of two regulatory (R) subunits (14). Cyclic AMP binding to the R subunit results in dissociation of the holoenzyme

[1] The abbreviations used are: PKA, protein kinase A; gPKA, giardial protein kinase A; PKAc, protein kinase A C subunit; PDB, Protein Data Bank; R, regulatory; C, catalytic; PCR, polymerase chain reaction; PKI, protein kinase A inhibitor peptide; PBS, phosphate-buffered saline; ORF, open reading frame; kb, kilobase pair(s).

with release of active C subunit. The activated C subunit of PKA can phosphorylate a number of intracellular proteins, including enzymes, cytoskeletal proteins, ion channels, and transcription factors (15). How the specific physiological effects of cAMP can be mediated by a broad spectrum protein kinase such as PKA is now being elucidated (16, 17). In a number of diverse cell types, PKA is localized in proximity to substrates by A kinase anchoring protein(s) that bind to both the R subunit and to a specific cell structure, often cytoskeletal (18). Targeting PKA to the proximity of phosphate acceptor protein molecules associated with specific cell structures can also achieve rapid responses to cAMP (16, 19).

Genes encoding three different C subunits and four different R subunits of PKA have been identified in humans (20). In higher eukaryotes, various combinations of R and C subunits display differences in tissue distribution (21–23), which may determine their functional specificity. The unique distribution and subcellular localization of PKA isoforms in higher eukaryotes may represent a functional interaction with nearby structures. In lower eukaryotes, three isoforms of PKA C subunit have been identified from *Drosophila melanogaster* (24), and from *Saccharomyces cerevisiae* (25). However, only one gene encoding PKA C subunit has been reported from *Caenorhabditis elegans*, *Dictyostelium discoidium*, *Leishmania major*, and *Trypanosoma cruzi* (26–29). *Dictyostelium* PKA plays a key role during differentiation and morphogenesis (30). Similarly, PKA plays critical roles in differentiation of *Leishmania* and *Trypanosoma* (28, 29). In contrast, *Saccharomyces* PKA appears to mediate cellular responses to various extracellular stimuli, including nutrients and heat shock (31).

Here we report the cloning and functional characterization of a giardial homologue of a PKA C subunit. Thus far, only a single isoform of gPKA C subunit has been identified in large scale sequencing efforts with ~3-fold coverage of the genome (32). Our studies demonstrate that, although the biochemical properties of the recombinant gPKA are largely similar to those of the mammalian enzyme, gPKA has some noteworthy structural differences. We found that cellular distribution of PKA was correlated with cell density and endogenous cAMP levels. At all cell densities, PKA localized to the eight flagellar basal bodies, which correspond to the centrosomes of higher eukaryotic cell (33). However, at low cell inocula and higher endogenous cAMP concentrations, PKA also localized to marginal plates along the intracellular portions of the anterior and caudal flagella. To our knowledge, this is the first indication of a role for cell signaling in giardial flagellar-associated structures. In addition, a PKA inhibitor greatly decreased giardial excystation. Thus, PKA may play a key role in regulating trophic behavior of the motile form, as well as cellular activation during excystation.

EXPERIMENTAL PROCEDURES

Materials—Unless specified, all materials were obtained from Sigma, Fisher, and Life Technologies, Inc.

Giardia Cell Culture and Differentiation—*G. lamblia* (WB clone C6, ATCC no. 50803) were maintained in TYI-S-33 medium with 10% bovine serum and bile (34). Encystation and excystation were induced essentially as described by Meng *et al.* (35). Briefly, encystation was induced by growing trophozoites for one culture cycle in TYI-S-33 medium without bile (pre-encystation). Bile-deficient medium was poured off along with unattached trophozoites and replaced with encystation medium containing 0.25 mg/ml porcine bile and 10 mM lactic acid, pH 7.8, and incubated at 37 °C for the time specified. Total encysting cultures were harvested at different time points by chilling and centrifugation and subsequently used for RNA and protein extraction. Cysts were harvested at 66 h by washing and incubating in cold double-distilled water to lyse any trophozoites or incomplete cysts (35). Excystation was induced by a two-step method that models cyst passage from the cold hypotonic freshwater external environment into the warm, acidic stomach, pH 4.0, 20 min, 37 °C (stage 1). Stage 2 models cyst passage from the stomach into the small intestine with exposure to slightly alkaline pH (8.0) and protease (1 mg/ml bovine trypsin type II) for 1 h at 37 °C. Cysts were pelleted at $8300 \times g$ and resuspended in growth medium for 60 min at 37 °C. Emerged motile trophozoites were enumerated using a hemocytometer. The percentage of excystation was calculated as the sum of the motile trophozoites and partially emerged trophozoites divided by the initial number of viable cysts.

Inhibition of Excystation—Myristoylated PKA inhibitor (amide 14-22, Calbiochem Novobiochem, San Diego, CA) was dissolved in water and diluted into water (pre-excystation) or excystation solutions. Inhibitor peptide was initially screened with the inhibitor present during 1 h before incubation at 4 °C and added again during stage 1 and 2 of excystation, since cysts were pelleted between stages. However, inhibitor was not included in the emergence step in growth medium because of possible effects on trophozoites. 50% inhibitory concentration (IC_{50}) was estimated by interpolation from concentration-inhibition curves. Viability was determined by trypan blue exclusion (35). To determine the stage(s) at which each inhibitor was effective, cysts were pre-incubated with inhibitor (at a higher than IC_{50} concentration, 10 μM) prior to stage 1 in water for 1 h at 4 °C, or during stage 1 or stage 2 of excystation.

The mean inhibition was normalized to solvent controls for each experiment. All experiments were repeated at least twice. Data shown are mean ($\pm$ S.D.) for at least two independent experiments. The *p* values were calculated by paired two-tailed Student's *t* test with the normalized comparison value set at 100% for control excystation (35).

PCR Amplification—A 250-base pair DNA fragment of PKA catalytic subunit was obtained by PCR amplification of *Giardia* genomic DNA using degenerate primers (upper primer, 5′-TAC(T)A(C)GXGAC(T)C(T)TXAAA(G)C(T)C-3′; lower primer, 5′-CCXAA(G)XG(C)A(C)(T)CCAC-CAA(G)TC-3′, where X is all four nucleotides). Primers were designed on the basis of the consensus sequence in the catalytic subdomains VIB and IX of the PKA catalytic subunit. Designed degeneracy allowed every possible codon for the consensus amino acid residues to maximize the probability of amplification. The amplified PKA fragment was purified, sequenced, and used to screen a *Giardia* cDNA library.

Screening of a cDNA Library—A *G. lamblia* WB clone C6 cDNA library was made in λZAPII (Stratagene, La Jolla, CA) using a kit (ZAP-cDNA^R synthesis kit, Stratagene) according to the manufacturer's protocol. The library was screened for the full-length clone of PKA using ^32P-labeled PKA probes as described previously (36). Five positive plaques were obtained by screening $\sim6 \times 10^5$ plaque-forming units. Positive plaques containing inserts were plaque-purified and inserts cloned into pBluescript plasmids by *in vivo* excision using ExAssist helper phage (Stratagene). Inserts were confirmed by restriction digestion and cross-hybridization.

DNA Sequencing and Identity Analysis—A capillary electrophoresis-based automated DNA sequencer (ABI Prism, 310 Genetic analyzer; ABI, Foster City, CA) was used to sequence positive clones from the cDNA library. A PCR-based reaction kit (ABI Prism™ dRhodamine Terminator Cycle Sequencing Ready Reaction), ABI prism 310 capillaries (61 cm $\times$ 50 μm, inner diameter) and POP-6 for long-read sequencing were used according to the manufacturer's protocol. Raw output was analyzed using ABI Prism sequence analysis software. The entire sequence identity was compared with the NCBI data base using PSI-BLAST. Multiple sequence alignment was done using MegAlign program from DNASTAR (Madison, WI) software. Tertiary structure was determined using SWISS-MODEL and Swiss-Pdb Viewer, an internet-based tool for automated comparative protein modeling (37, 38).

Southern Blot and Northern Blot—Genomic DNA from *Giardia* was isolated using standard protocol as described by Maniatis *et al.* (39). Total RNA was extracted using an RNA isolation kit (Stratagene) according to the manufacturer's specification. ^32P-Labeled gPKA cDNA probes were used for hybridization as described previously (36). For Northern blots, a strand-specific probe was synthesized and used as a probe for gPKA. Briefly, 25–50 ng of the template DNA was labeled using 100 pmol of antisense primer, [^32P]dCTP, dNTP, and Klenow (exo−) (Stratagene). Unincorporated nucleotides were removed using a NucTrap push column (Stratagene).

Expression and Purification of Recombinant gPKA—The gPKA ORF was cloned into a T7 polymerase-driven expression vector pET30Ek/LIC (Novagen, Madison, WI) according to the manufacturer's protocol. Two primers (upper primer, 5′-GACGACGACAAGATGGAAGATAT-TCAAGTA-3′; and lower primer, 5′-GAGGAGAAGCCCGGTCTATTTA-AATCCCAC-3′) were designed to amplify the PKA ORF (1.08 kb) and part of the vector sequence. The PCR product was treated with T4 DNA polymerase and dATP only to use the exonuclease activity of the po-

lymerase to generate vector compatible overhangs. Pre-digested vector and insert were annealed and used to transform BL21 (DE3) *Escherichia coli* cells. Induction of gPKA overexpression in BL21 (DE3) was performed at 25 °C with 0.5 mM isopropyl-1-thio-β-D-galactopyranoside. Expressed gPKA as a 47-kDa His tag and S tag fusion protein was purified through His-Bind columns (Novagen) and used as antigen for generation of polyclonal antibodies through a commercial vendor (Co-Calico, Reamftown, PA). The His tag and S tag sequences added 6 kDa of molecular mass to the fusion protein.

Western Blot and Immunodepletion Experiment—Trophozoites and encysting cells were harvested, and total proteins (50 μg) were used for the immunodetection of gPKA using the polyclonal antibody made against recombinant protein. A chemiluminescence detection kit (Pierce) was used to detect positive signals recognized by anti-gPKA antibody using anti-rabbit HRP-conjugated secondary antibody.

Immunodepletion was done in a two-step process. Crude trophozoite extracts (500 μg) in 100 mM Tris, pH 7.5 and 5 mM MgCl$_2$ were diluted in TAN buffer (10 mM Tris acetate, pH 8.0, 1% Nonidet P-40, 100 mM NaCl) containing 1 mM sodium orthovanadate, 1 mM phenylmethylsulfonyl fluoride, 2 mM *n*-ethylmalemide, 1 μg/ml leupeptin, and 2 μg/ml aprotinin. Ten μg of rabbit IgG was added to the extract and incubated for 2 h at 4 °C to remove nonspecific binding of proteins to gPKA IgG. Next, 150 μl of Protein A-agarose beads (50% slurry) was added and incubated overnight at 4 °C to remove rabbit IgG. Protein A beads were separated next by centrifuging at 1,500 × *g* for 5 min at 4 °C. The supernatant was incubated with 50 μg of gPKA antibody for 6 h at 4 °C followed by 200 μl of Protein A beads for 18 h at 4 °C. Protein A beads were separated by centrifugation, and the supernatant was used for the kinase assay.

Assay of PKA Activity—Trophozoites were grown to confluence, harvested at 700 × *g*, and washed three times with PBS. They were lysed in a medium containing 100 mM Tris, pH 7.5, and 5 mM MgCl$_2$ and a mixture of protease inhibitors (Sigma) using a French press (750 p.s.i.). The lysate was centrifuged at 30,000 × *g*, and the supernatant was passed through a syringe filter (0.45 μm). The filtrate was used for the kinase assay using kemptide (Calbiochem-Novobiochem Corp) as a substrate. Fifty μg of crude extract or purified recombinant gPKA (5 μg) was used in a reaction mix containing 100 mM Tris, 5 mM MgCl$_2$, 0.2 mM ATP, 0.2 mM kemptide, and 0.5 nM [γ-^{32}P]ATP. The reaction mix was incubated at 30 °C for 10 min and spotted (40 μl) on phosphocellulose filter discs. Filters were washed four times for 5 min each with 1% phosphoric acid and bound radioactivity counted in a liquid scintillation counter (LKB). Kinase assays using recombinant gPKA were conducted in the presence or absence of the myristoylated PKA inhibitor 14-22 amide and a PKA-specific hexamer inhibitor (RGYALG) (Bachem) at different concentrations. Assays using crude extract were performed in the presence or absence of 4 μM cAMP (Calbiochem). The catalytic parameters were measured under standard assay condition, and the data were graphically fit to the Lineweaver-Burk form of the Michaelis-Menten equation (40).

Immunofluorescence Analysis—*G. lamblia* trophozoites were inoculated in growth medium at 350–2000 cells/ml in 12-well tissue culture plates and allowed to grow and attach to 18-mm glass coverslips for 65–70 h in an AnaeroPack jar (Mitsubishi Gas Chemical Company, Inc., Japan) at 37 °C. Coverslips containing attached trophozoites were directly fixed in 100% chilled MeOH (−20 °C) for 10 min at −20 °C and further permeabilized with PBS containing 0.5% Triton X-100 for 10 min. Permeablized trophozoites were blocked for 1 h in blocking buffer (5% goat serum, 1% glycerol, 0.1% BSA, 0.1% fish gelatin, and 0.04% sodium azide in PBS), and incubated with rabbit anti-gPKA polyclonal antibodies (1/2500 in blocking buffer) and/or mouse monoclonal anti-centrin antibodies (clone 20H5, 1/500 in blocking buffer) (41) for 1 h. At the end of incubation, cells were washed for 5 min (four times) with PBS and incubated with the secondary antibodies (anti-rabbit ALEXA 488 and/or anti-mouse ALEXA 568 (Molecular Probes, Eugene, OR) each diluted in blocking buffer 1/800) for 1 h. Next, cells were washed for 5 min (four times) with PBS, post-fixed for 7 min with 4% paraformaldehyde (Electron Microscopy Sciences, Ft. Washington, PA) in PBS, rinsed with PBS, and mounted on glass slides in Prolong (Molecular Probes). Localization of gPKA and centrin was observed on a Zeiss LSM 510 laser scanning confocal microscope equipped with argon-krypton (455/488) and helium-neon (543/633) lasers and appropriate filter sets.

cAMP Measurements—To measure endogenous cAMP levels in various stages of *G. lamblia* growth, a competitive cAMP enzyme immunoassay (Biotrack Cellular Communications Assays, Amersham Pharmacia Biotech) was employed. *G. lamblia* were cultured as described for immunolocalization. Using the nonacetylated protocol 3 method of the Biotrack enzyme immunoassay, parasites were lysed in a 500-μl vol-

ume of lysis reagent and the amount of cAMP was determined by the manufacturer's protocol. The enzyme immunoassay was repeated five times with parasites from independent cultures, and cAMP measurements were done in duplicate for each sample. Mean differences in the amount of cAMP levels between different cell densities were compared using a paired Student's *t* test, and *p* values ≤ 0.05 were considered significantly different.

RESULTS

Sequence and Expression Analyses of gPKA—Upon screening a *Giardia* cDNA library with a 250-base pair probe derived from conserved PKA sequences, a 1.28-kb fragment containing an ORF of 1.08 kb (360 amino acids) corresponding to a *Giardia* homologue of PKA catalytic subunit was cloned (Fig. 1). An unusually long 189-base pair 3′-untranslated region was present in the cloned fragment (accession no. AF181097).

The translated amino acid sequence of the ORF showed 48% identity with *E. gracilis,* 45% identity with *C. elegans,* 43% identity with human, and 41% identity with yeast cyclic AMP-dependent PKA catalytic subunit with probability scores between 3e-77 and 2e-69 as obtained from PSI-BLAST homology search of the NCBI data base. Since the serine-threonine kinase family exhibits a significant degree of conservation of the kinase domains, the gPKA ORF also showed limited homology with a number of other serine threonine kinases, such as cGMP-dependent protein kinases. However, probability scores (starting at 2e-57 for human KGPA) were significantly lower, and gPKA does not have a cyclic GMP-binding domain.

The identification of the ORF as a PKA homologue was strengthened by the presence of most of the key functional motifs, as predicted by comparison with the crystal structure of bovine PKA C subunits (PKAc) (42). The amino acid sequence analysis of gPKA shows the presence of all 11 subdomains of the kinase domain of PKAc (Fig. 1). Because of its early evolutionary position (43), giardial genes are frequently highly divergent (8). Despite the lower degree of identity, gPKA exhibits the important consensus motifs, which include the glycine-rich consensus motif G*X*G*XX*G*X*V (Gly-24 to Val-31 using the amino acid numbers of the giardial sequence) in subdomain I, the APE (Ala-190 to Glu-192) motif in subdomain VIII and the catalytic loop YRDLK*XX*N (Tyr-138 to Asn-145) in subdomain IV. The glycine loop is involved in interactions with ATP β-phosphate oxygens and the pseudosubstrate peptides such as the PKA inhibitor peptide (PKI). The APE motif helps to stabilize the large C-terminal lobe of PKAc. Highly conserved amino acid residues such as Lys-46 in subdomain II, which is responsible for ATP-binding; Glu-65 in subdomain III, which interacts with Lys-46; and Arg-264 in subdomain IX are also present. Among the consensus residues for interaction with the R subunit of PKA or PKI, only His-61 in subdomain III, Arg-107 (not conserved in PKAcγ), and Arg-108 in subdomain V are present but Trp-196, Thr-197, Leu-198, and Lys-213 (in vertebrates) in subdomain VIII are not. The consensus residue Thr-197 (in vertebrates) that is responsible for autophosphorylation in other species is replaced by a serine residue, which can also be phosphorylated in gPKA (Ser-181). In subdomain VII, the Phe residue in DFG sequence is also substituted by another hydrophobic residue Leu in gPKA. This triplet helps to orient γ phosphate for transfer to the substrate by chelating the Mg^{2+} ion, which bridges the β and γ phosphates of the ATP. The invariant Arg-280 (Arg-264 in gPKA) responsible for stabilizing the large lobe of PKAc is also present.

Analyses of Southern blots and large scale genomic sequence (32) suggests that gPKA is a single-copy gene. Northern and Western analyses showed that gPKA was expressed apparently at a constant concentration during both growth and encystation as a 1.3-kb transcript and a 41-kDa protein (data not shown).
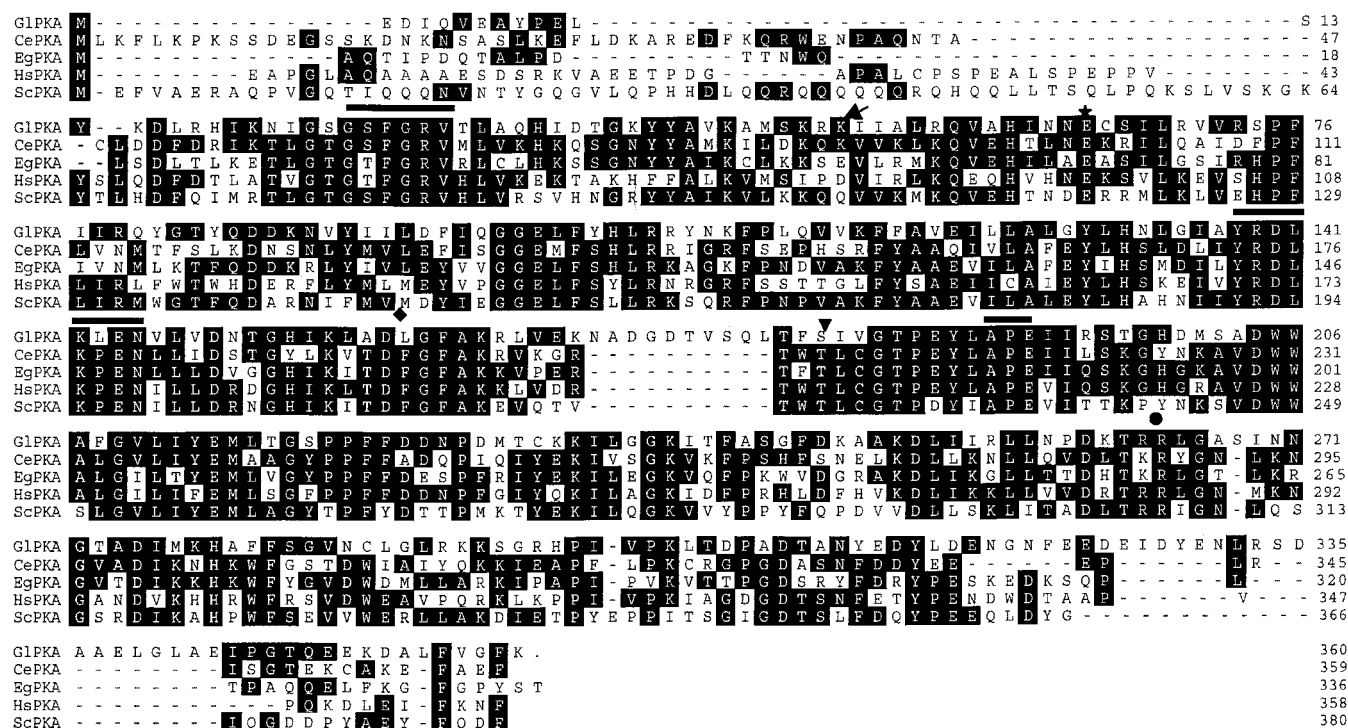
```
GlPKA  M- - - - - - - - - - - - - - - - - EDIQVEAYPEL- - - - - - - - - - - - - - - - - - - - - - - - - - - - - - - - - - - - - - S  13
CePKA  MLKFLKPKSSDEGSSKDNKNSASLKEFLDKAREDFKQRWENPAQNTA- - - - - - - - - - - - - - - - - - - - -  47
EgPKA  M- - - - - - - - - - - - - - - AQTIPDQTALPD- - - - - - - - TTNWQ- - - - - - - - - - - - - - - - - - - - - - - - - - - -  18
HsPKA  M- - - - - - - - - EAPGLAQAAAAESDSRKVAEETPDG- - - - - APALCPSPEALSPEPPV- - - - - - - - -  43
ScPKA  M-EFVAERAQPVGQTIQQQMVNTYGQGVLGPHHDLQQRQQQQQQQRQHQQLLTSQLPQKSLVSKGK  64

GlPKA  Y- - KDLRHIKNIGSGSFGRVTLAQHIDTGKYVKAMSKRKIIALRQVAHINNECSILRVVRSPF  76
CePKA  -CLDDFDRIKTLGTGSFGRVTMLAQHKQSGNYYAMKILDKQKVVKLKQVEHTLNEKRILQAIDFPF  111
EgPKA  - -LSDLTLKETLGTGTFGRVRLCLHKSSGNYYAIKCLKKSEVLRMKQVEHILAEASILGSIRHPF  81
HsPKA  YSLQDFDTLATVGTGTFGRVHLVKEKTAKHFALKVMSIPDVIRLKQEQHVHNEKSVLKEVSHPF  108
ScPKA  YTLHDFQIMRTLGTGSFGRVHLVRSVHNGRYYAIKVLKKQQVVKMKQVEHTNDERRMLKLVEHPF  129

GlPKA  IIRQYGTYQDDKNVYIILDFIQGGELFYHLRRYNKFPLQVVKFFAVEILLALGYLHNLGIAYRDL  141
CePKA  LVNMTFSLKDNSNLYMVLEFISGGEMFSHLRRIGRFSEPHSRFYAAQIVLAFEYLHSLDLIYRDL  176
EgPKA  IVNMLKTFQDDKRLYIVLMEYVVGGGELFSHLRKDVAKFYAAEVILAFEYIHSMDILYRDL  146
HsPKA  LIRLFWTWHDERFLYMLMEYVPGGELFSYLRNRGRFSSTTGLFYSAEIICAIEYLHSKEIVYRDL  173
ScPKA  LIRMWGTFQDARNIFMVMDYIEGGELFSLLRKSQRFPNPVAKFYAAEVILALEYLHAHNIIYRDL  194

GlPKA  KLENVLVDNTGHIKLADLGFAKRLVEKNADGDTVSQLTFSIVGTPEYLAPEIIRSTGHDMSADWW  206
CePKA  KPENLLIDSTGYLKVTDFGFAKRVKGR- - - - - - - - - -TWTLCGTPEYLAPEIILSKGYNKAVDWW  231
EgPKA  KPENLLLDVGHIKITDFGFAKKVPER- - - - - - - - - -TFTLCGTPEYLAPEIVQSKGHGKAVDWW  201
HsPKA  KPENILLDRDGHIKLTDFGFAKKLVDR- - - - - - - - - -TWTLCGTPEYLAPEVIQSKGHGRAVDWW  228
ScPKA  KPENILLDRNGHIKITDFGFAKEVQTV- - - - - - - - - -TWTLCGTPDYIAPEVITTKPYNKSVDWW  249

GlPKA  AFGVLIYEMLTGSPPFFDDNPDMTCKKILGGKITFASGPDKAAKDLIIRLLNPDKTRRLGASINN  271
CePKA  ALGVLIYEMAAGYPPFFADQPIQIYEKIVSGKVKFPSHFSNELKDLLKNLLQVDLTKRYGN-LKN  295
EgPKA  ALGILTYEMLVGYPPFFDESPFRIYEKILEGKVQFPKWVDGRAKDLIKGLLTTDHTKRLGT-LKR  265
HsPKA  ALGILIFEMLSGFPPFFDDNPFGIYQKILAGKIDFPRHLDFHVKDLIKKLLVVDRTRRLGN-MKN  292
ScPKA  SLGVLIYEMLAGYPYFQDTTPMKTYEKILQGKVVYPPYFQPDVVDLLSKLITADLTRRIGN-LQS  313

GlPKA  GTADIMKHAFFSGVNCLGLRKKSGRHPI-VPKLTDPADTANYEDYLDENGNFEEDEIDYENLRSD  335
CePKA  GVADIKNHKWFGSTDWIAIYQKKIEAPF-LPKCRGPGDASNFDDYEE- - - - -EP- - - - - -LR- -  345
EgPKA  GVTDIKKHKWFYGVDWDMLLARKIPAPI-PVKVTTPGDSRYFDRYPESKEDKSQP- - - - - -L- - -  320
HsPKA  GANDVKHHKWFRSVDWIAVPQRKLKPPI-VPKIAGDGDTSNFETYPENDWDTAAP- - - - - - -V- -  347
ScPKA  GSRDIKAHPWFSEVVWERLLAKDIETPYEPPITSGIGDTSLFDQYPEEQLDYG- - - - - - - - - - -  366

GlPKA  AAELGLAEIPGTQEEKDALFVGFK.  360
CePKA  - - - - - - - - ISGTEKCAKE-FAEF  359
EgPKA  - - - - - - - -TPAQQELFKG-FGPYST  336
HsPKA  - - - - - - - - - - PQKDLEI-FKNF  358
ScPKA  - - - - - - - -IQGDDPYAEY-FQDF  380
```

FIG. 1. **Multiple sequence alignment of gPKA.** *Gl*, *G. lamblia*; *Ce*, *C. elegans*; *Eg*, *E. gracilis*; *Hs*, *H. sapiens*; *Sc*, *S. cerevisiae*. The *solid bars* above the sequences indicate the G loop, catalytic loop, and APE sites, respectively. The *black arrow* indicates the conserved Lys-64 for ATP binding. The *asterisk* indicates conserved Glu-65, which interacts with Lys-46. The *triangle* shows Ser-181 instead of Thr-197 required for autophosphorylation in other species. The *diamond* shows Leu instead of Phe in sequence DFG, and the *filled circle* shows Arg-264.

gPKA Has a Predicted Additional Loop in the Activation Domain—Using an internet-based protein modeling program (37, 38), we compared the three-dimensional structure of gPKA to the α-catalytic subunit of bovine PKA complexed with the inhibitor staurosporine (PDB accession no. 1STC) and H8 protein kinase inhibitor (PDB accession no. 1YDS) (Fig. 2*A*). However, this is a predicted three-dimensional structure based on the actual crystal structure of the template complexed with inhibitors, which may contribute some degree of inaccuracy. Nonetheless, the superimposed structure of gPKA indicates two major differences. A small loop (*red*) is in subdomain XI at the C-terminal end of the kinase domain (Fig. 2, *A* and *B*). The interaction of the invariant arginine corresponding to Arg-280 (Fig. 2*B*, *yellow arrow*), which stabilizes the large lobe by forming an ion pair with Glu-208 is predicted to be present in gPKA (Arg-254 and Glu-182) but the hydrogen (H) bond between Arg-280 and Asn-283 appears to be missing in gPKA. Asn-283, which maintains the loop structure by forming a H-bond with Leu-277 in the template, is replaced by Ser-258 forming a H-bond with Lys-251 in gPKA, thus making the loop more relaxed than that in the template.
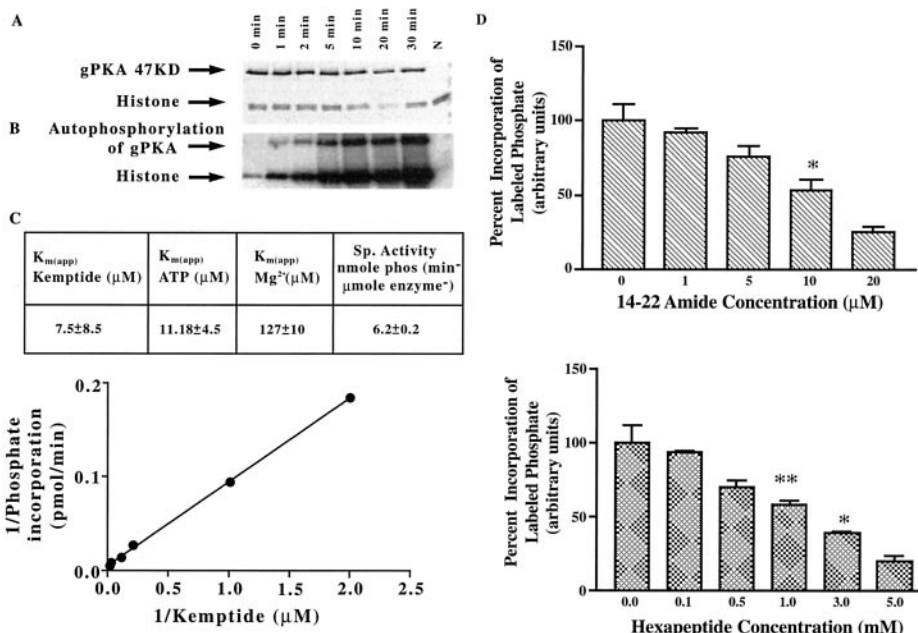
The other major difference is the large loop in the activation domain (subdomain VIII shown in *red* in Fig. 2 (*A*, *C*, and *D*)). A unique stretch of 10 amino acids from Asn-169 to Leu-178, is predicted to form an additional loop creating a distinct change in the conformation of the activation domain (Fig. 2, *C* and *D*). Specifically, Ser-171 (Thr-197 in the template) does not form H-bonds with Lys-153 (Lys-189) and Thr-169 (Thr-195), which are present in the crystal structure of the 1YDS template. These ion pairs may stabilize the subdomain VIII in an active conformation, thereby permitting proper orientation of the substrate peptide. The presence of several H-bonds in the extra loop indicates a highly stable configuration, which may interfere with the binding of the PKI inhibitor. The Mg^{2+} binding domain DFG (Asp-184 to Gly-186), although replaced by DLG (Asp-148 to Gly-150) in gPKA shows a similar conformation

with H-bond formation between Leu-149 and Ala-152 (Fig. 2*C*). Another minor difference is in the subdomain IX representing the large α-helix in the large lobe (Fig. 2*E*). The invariant Asp-220 (Asp-194 in gPKA), which acts to stabilize the YRD-K*XX*N catalytic loop by forming H-bonds with backbone amides of Arg-165 and Tyr-164 is predicted to form H-bond only with Arg-129 but not with Tyr-128 in gPKA. This may cause instability in loop formation.

Recombinant gPKA Is Catalytically Active—We determined the catalytic activity of the purified recombinant gPKA using histone (Fig. 3) and kemptide (see below) as substrates. Kemptide is a synthetic heptapeptide (LRRASLG) and is highly specific for PKA. Recombinant gPKA phosphorylated both substrates (specific activity 6.2 ± 0.2 nmol of phosphate/min/μmol of enzyme) and was also capable of autophosphorylation (Fig. 3, *A* and *B*). Purified gPKA autophosphorylated in a concentration dependent manner with a stoichiometry of 1–1.8 mol of phosphate/mol of gPKA. Phosphorylated PKA increased with incubation time and was not observed in the control lane without enzyme. The recombinant PKA band is also absent from the control no extract lane in the protein gel (Fig. 3*A*). Apparent K_m values for Mg^{2+}ATP and kemptide are in the micromolar range: kemptide (7.5 ± 8.5 μM), Mg^{2+} (127 ± 10 μM), and ATP (11.18 ± 4.5 μM as phosphate donor). The apparent K_m for ATP and the synthetic peptide kemptide are in the range close to that of cytosolic type II PKA from erythrocyte and from bovine heart (44, 45). The K_m for Mg^+ for gPKA is in the micromolar range instead of the millimolar range that has been reported for vertebrate PKAc (42). Additionally, Mg^{2+} is preferred over Mn^{2+} as the divalent cation and ATP over GTP as the phosphate donor for optimum activity (data not shown). Kinase activity of recombinant gPKA with histone or kemptide was not inhibited by the 6-22 amide (PKI), which is potent inhibitor of mammalian PKAs (data not shown). However, both the shorter myristoylated peptide inhibitor, 14-22 amide (which inhibited giardial excystation, see below) and a PKA-specific synthetic
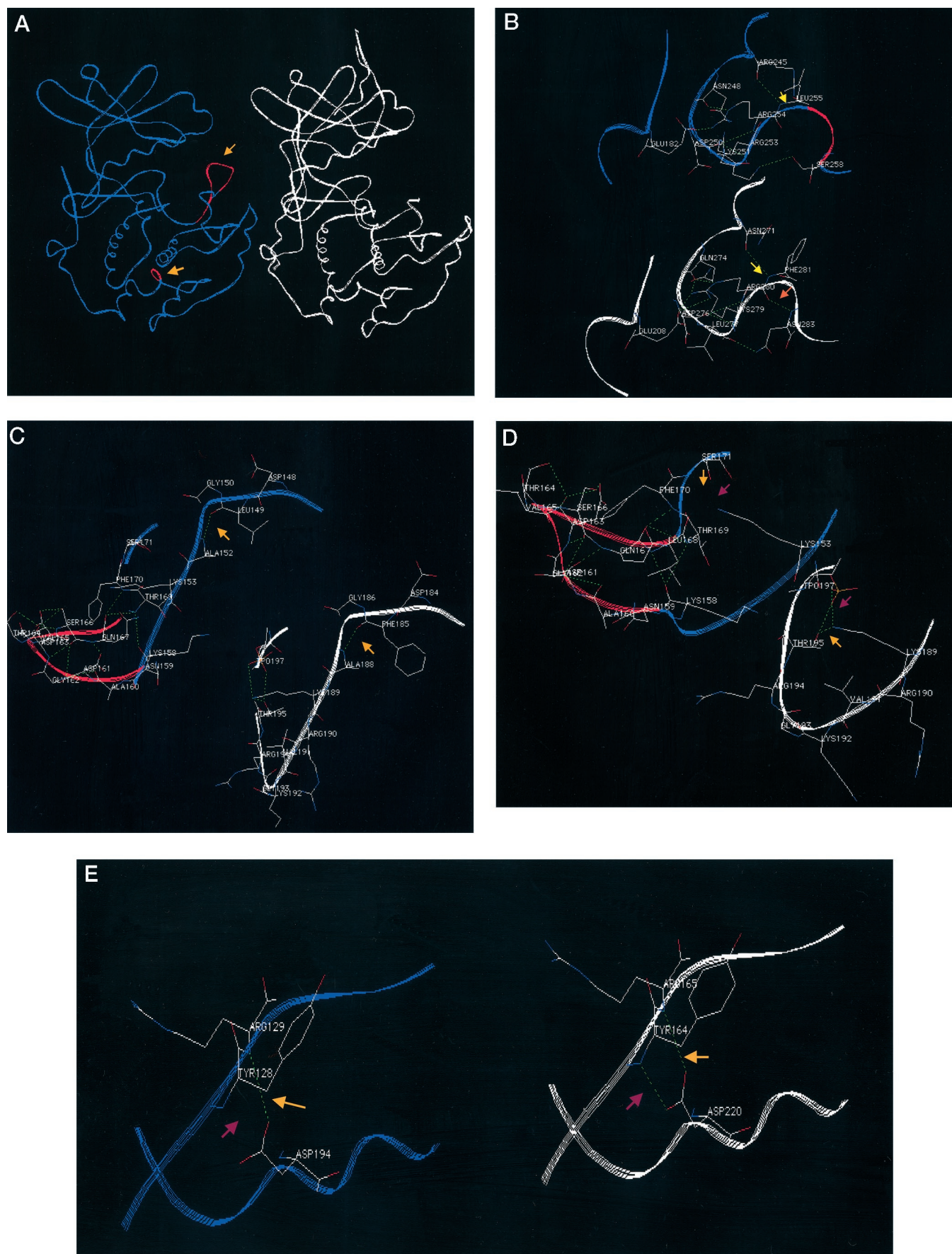
FIG. 3. **Phosphorylation of histone by gPKA at different incubation time (0–30 min).** *A*, Coomassie Blue-stained gel showing equal amounts of histone and gPKA in all lanes except in *lane N*. *N* contains histone but no extracts. *B*, autoradiogram showing phosphorylated histone and gPKA. *C*, Lineweaver-Burk plot of the phosphorylation of kemptide by gPKA at 30 °C. Each *point* represents the mean of three separate experiments. Apparent K_m for kemptide, ATP, and Mg^{2+}, and specific activity of gPKA are presented in the *box*. *D*, inhibition of phosphorylation of kemptide by myristoylated PKA inhibitor 14-22 and by the synthetic hexapeptide inhibitor (RGYALG). Data represented as mean ± S.D. (* indicates $p < 0.03$ ($n = 3$) for the myristoylated inhibitor and $p < 0.005$ ($n = 2$) for the hexapeptide; ** indicates $p < 0.04$).

$K_{m(app)}$ Kemptide (μM)	$K_{m(app)}$ ATP (μM)	$K_{m(app)}$ Mg^{2+}(μM)	Sp. Activity nmole phos (min⁻¹ μmole enzyme⁻¹)
7.5±8.5	11.18±4.5	127±10	6.2±0.2

hexapeptide inhibitor (RGYALG) were able to inhibit phosphorylation of kemptide by gPKA with IC_{50} values of 10 μM (Fig. 3*D*) and 3 mM, respectively. The IC_{50} of the hexapeptide inhibitor was lower than that obtained with the PKA from rabbit skeletal muscle (46).

Catalytically Active PKA Is Present in Giardia Trophozoites—We measured the phosphorylating ability of the native PKA in the crude extracts of trophozoites using kemptide as the specific substrate (Fig. 4). PKA activity was monitored in the presence or absence of kemptide (Fig. 4*B*) to eliminate phosphorylation of endogenous substrates by PKA and other kinases. A 5-fold increase in activity was obtained with kemptide, indicating active gPKA in the trophozoite extracts (specific activity 1.2 ± 0.26 nmol/min/mg of protein). Exogenous cAMP at a concentration (4 μM) slightly higher than that used for the mammalian PKA was able to stimulate gPKA activity in the crude extract. A 2.5-fold increase in kemptide phosphorylation was noted following addition of cAMP in the crude extract ($p < 0.02$) (Fig. 4*C*). To confirm that the activity was due to native PKA, we immunodepleted gPKA from crude trophozoite extracts by immunoprecipitation using a rabbit polyclonal antibody against recombinant gPKA. The specificity of the gPKA antibody was shown by its reaction with the 47-kDa recombinant gPKA and with a single 41-kDa polypeptide in the crude extract in Western blot at a dilution of 1:7000 (Fig. 4*A*). The idea that the cAMP-stimulated posphorylation of kemptide in crude extracts was due to gPKA was also supported by immunodepletion studies. As expected, addition of kemptide did not increase kinase activity of the depleted crude extract (Fig. 4*B*). Depletion of the native PKA was confirmed by Western blot

analysis, which shows no PKA protein band in the depleted lane (Fig. 4*A*). The higher band in this lane is the residual PKA IgG that reacted with anti-rabbit secondary antibody.

Immunolocalization of gPKA and cAMP Measurements in Trophozoites—The cellular localization of PKA enzyme in *G. lamblia* trophozoites was determined using primary antiserum generated to purified recombinant *Giardia* PKA (or anti-gPKA) and confocal microscopy. At low cell densities (achieved with inocula of 350–700 cells/ml), distinct signals were seen in dense rods or marginal plates along the intracellular portions (axonemes) associated with the pairs of anterior and caudal flagella, as well as in the eight basal bodies located between the nuclei (Fig. 5*A*). Localization of gPKA to the flagellar basal bodies was confirmed by colocalization with monoclonal anti-centrin antibody (41) (Fig. 5*B*). In addition to the basal bodies, anti-centrin localized along the two axonemes associated with the posterior-lateral flagella that were not recognized by gPKA (Fig. 5*B*). Neither antibody reacted in the region of the ventro-lateral pair of flagella. Localization of gPKA at high cell density (inoculum > 1400 cells/ml) also showed staining of basal bodies. However, there was no localization to axonemes and diffuse staining was observed in the cytosol (Fig. 5*C*). Refeeding cells from the higher inocula cultures with fresh medium for 10 min, led to the localized patterns (Fig. 5*A*); however, exposure to exogenous dibutyryl cAMP did not (data not shown). Results from the cAMP analyses showed that those cells having a diffuse staining pattern (Fig. 5*C*) had significantly ($p < 0.03$ for comparisons of 700 with 1400 and 2000 cells/ml) lower endogenous levels of cAMP compared with those parasites with localized staining (Fig. 5*A*) to flagellar marginal plates compo-

Fig. 2. **Analysis of predicted three-dimensional structure of gPKA.** *A*, comparison of the predicted three-dimensional structure of gPKA (*blue*) and crystal structure of the α-catalytic subunit of bovine PKA complexed with staurosporine (*white*). Structures of gPKA and the template are represented as *blue* and *white ribbons*, respectively. Any change in the color of the *blue ribbon* represents dissimilarities with the template. Increasing color intensity represents increasing degree of mismatches leading to *red* representing absolute differences between gPKA and the template. *Arrows* indicate the additional loop structure in gPKA. *B*, comparison of the structure of the loop in subdomain IX. *Blue*, gPKA; *white*, α-catalytic subunit of bovine PKA complexed with H8 inhibitor peptide (PDB accession no. 1YDS). *Yellow arrows* indicate the invariant Arg-280 (Arg-254 in gPKA). *Red arrow* indicates the H-bond that is missing from gPKA. *C*, comparison of the activation domains of gPKA (*blue*) and bovine PKAc-α (*white*). The *orange arrow* indicates the H-bond in the Mg^{2+}-binding domain when Phe-185 is replaced by Leu-149 in gPKA. *D*, structures of the activation domains of gPKA (*blue*) and bovine PKAc-α complexed with H8 inhibitor peptide (*white*). *Orange arrows* indicate H-bonds that are missing between Lys-153 and Thr-165 and between Lys-153 and Ser-171 (Lys-189 and Thr-195, and Lys-189 and Thr-197 in bovine PKAc) making the loop more relaxed. *Purple arrows* show the bond that is missing between Thr-165 and Ser-171 (Thr-195 and Thr-197 in bovine PKAc). *Red loop* indicates several H-bonds that are absent in bovine PKAc. *E*, comparison of the subdomain IX of gPKA (*blue*) and bovine PKAc-α (*white*). *Orange arrows* indicate the invariant Asp-194 (Asp-220 in bovine PKAc). *Purple arrows* indicate the H-bond that is missing between Asp-194 and Tyr-128 (Asp-220 and Tyr-164 in bovine PKAc) needed to stabilize the catalytic loop.

FIG. 4. **Detection of active gPKA in trophozoite extracts.** *A*, Western blot. Detection of gPKA in trophozoite extracts before and after immunodepletion of gPKA by PKA antibody. The PKA IgG band in the depleted extract lane is the remaining gPKA antibody recognized by the anti-rabbit secondary antibody. *B*, kinase activity in crude extracts and immunodepleted extracts using kemptide as the substrate. Data represented as mean $\pm$ S.D. ($n = 3$). *C*, effect of exogenous cAMP on the kinase activity in the crude extract. Data represented as mean $\pm$ S.D. ($p < 0.02$, $n = 4$).
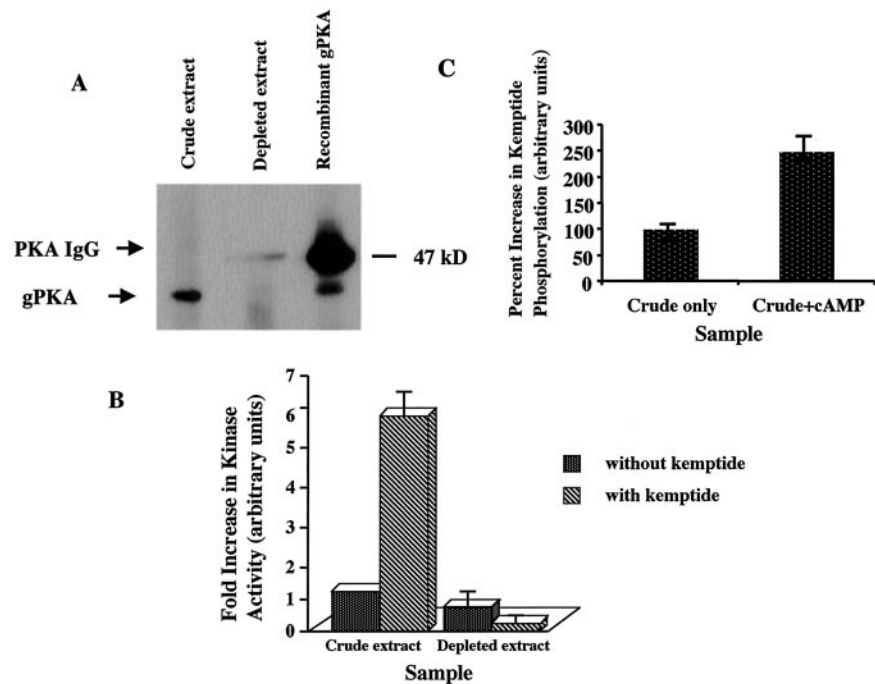
nents (Fig. 5*D*). This suggests that localization of gPKA to the flagella is responsive to both cell density and growth factors.

Involvement of gPKA in the Excystation Process—Since excystation is a very rapid differentiation in response to extreme changes in the external milieu, intracellular signaling may be more important than changes in gene expression. Cyclic AMP is important in cellular differentiation in other organisms, and we asked if PKA activity might be needed for excystation. We found that a cell-permeable myristoylated pseudosubstrate inhibitor specific for PKA (amide 14-22) inhibited excystation with an IC_{50} of 3 μM when it was present throughout excystation (Fig. 6*A*). The effect of the PKA inhibitor on the individual stages of excystation was also studied. Pre-incubating cysts with the PKA inhibitor prior to excystation stimuli was effective in preventing excystation. The inhibitor was also effective at the low pH stage 1, which mimics passage through the stomach, but less effective at stage 2, which mimics cyst entry into the host small intestine (Fig. 6*B*). Since this stage entails digestion of cysts with trypsin, it is likely that the peptide inhibitor was at least partly inactivated. These studies suggest a need for PKA activity during the early stages of excystation.

DISCUSSION

Since PKA regulates critical cellular processes in both higher and lower eukaryotes, we characterized a homologue of a PKA catalytic subunit of *Giardia*. Sequence and structural predictions showed that most of the kinase subdomains that are conserved in higher eukaryotes, are present in gPKA, and we have also identified a regulatory subunit homologue (data not shown), suggesting a conventional PKA holoenzyme. Despite several structural differences, functional characterization demonstrates that both recombinant and native PKA are catalytically active and phosphorylate a PKA-specific substrates, such as kemptide as well as histone. Structural alignments, substrate specificity, and stimulation of the kinase activity of native PKA by cAMP all suggest that the cloned ORF is indeed a *Giardia* homologue of the C subunit of PKA.

In the case of a ubiquitous enzyme, such as PKA, it is important to understand how different physiological conditions determine specificity. A prominent level of control is to localize signaling proteins to specific subcellular organelles or compart-

ments. Thus, it is very interesting that, in *Giardia*, PKA can localize to both basal body/centrosome and specific flagellar structures. In certain cells, protein kinase A-anchoring proteins or AKAPs can bind to a PKA regulatory subunit, which then localizes the catalytic subunit to the proper structure. For example, AKAP450 targets PKA to centrosomes in HeLa cells (47). In bovine and human sperm, mAKAP82 localized PKA, via its RII subunit, to the fibrous sheath (48), between the axoneme and the surrounding mitochondrion. In contrast, PKA of a single-celled flagellated alga, *Chlamydomonas*, is reported to be localized to the radial spokes of the flagellar structure, where it may be involved in regulating dynein ATPase (49). The location of PKA in giardial flagellar structure appears closer to that of mammalian sperm than to that of *Chlamydomonas*.

Immunolocalization of gPKA in trophozoites showed a selective accumulation of PKA in the eight flagellar basal bodies at low and high cell densities. Localization of PKA to the basal bodies was confirmed by colocalization with centrin, a basal body-specific Ca^{2+}-binding protein. Basal bodies are rodlike structures associated with the origins of the flagellar axonemes and are involved in cell motility. The basal bodies of flagellated cells correspond to the centrosomes of higher eukaryotic cells (50). Centrin, which is found in centrosomes in higher eukaryotes and basal bodies of all flagellated and ciliated cell types including *Giardia* (51), is also involved in mitotic spindle pole segregation in *Saccharomyces* (52). Interestingly, sequence analyses have shown that a giardial centrin gene has a motif that predicts phosphorylation by PKA. Indirect immunofluorescence studies revealed that antibody specific for phosphorylated centrin reacted with the basal bodies of dividing cells, but not interphase cells.[2] Thus, centrin in the basal bodies may be a substrate for phosphorylation by PKA during a specific stage of the cell cycle. In contrast, gPKA was associated with the paired anterior and caudal flagella only at low cell densities, which correlated with higher endogenous cAMP levels. This is the first evidence that trophozoites can respond to signals from their environment with changes in cAMP levels

---

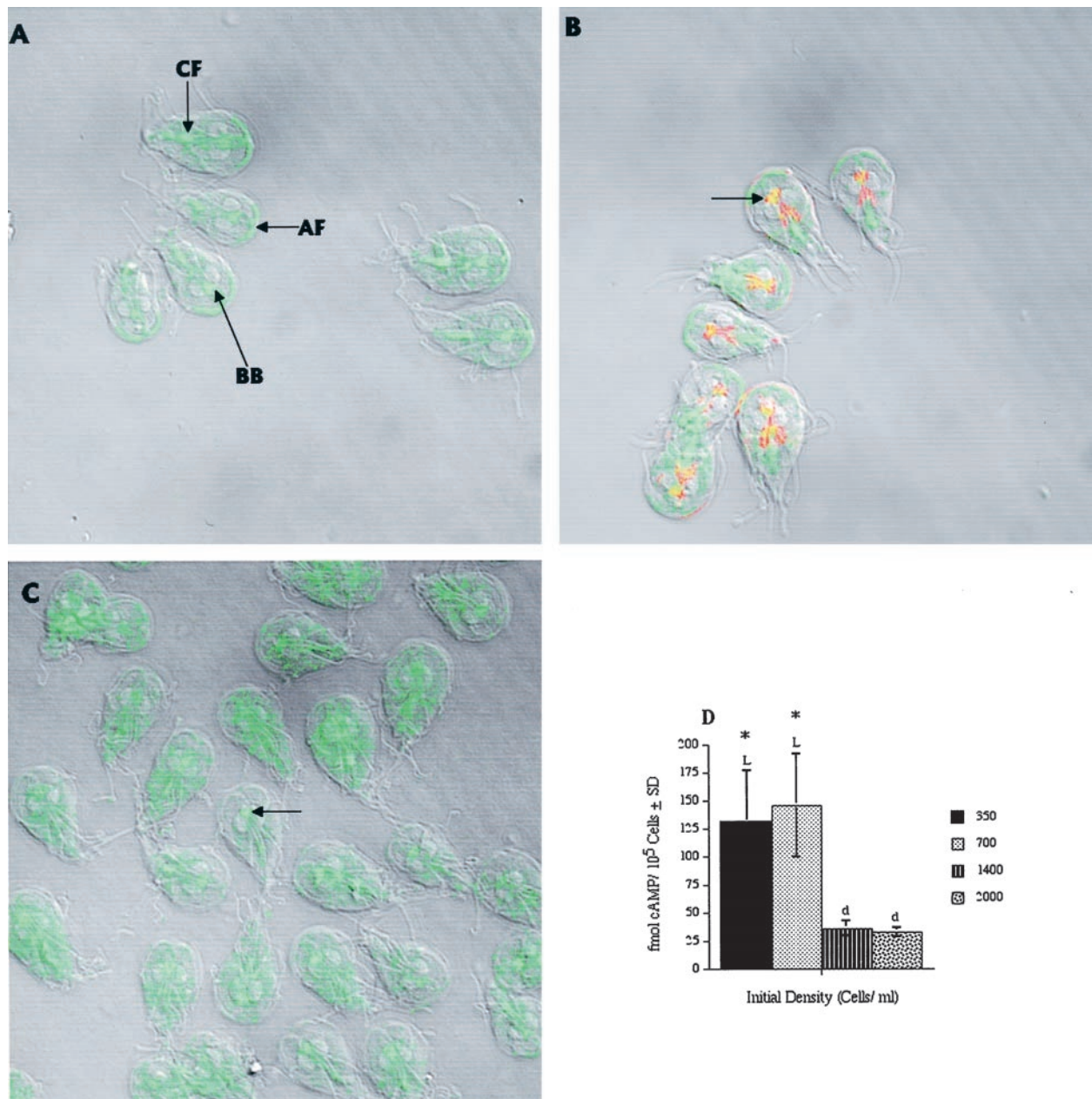[2] W. L. Lingle and J. L. Salisbury, personal communication.

FIG. 5. **Immunolocalization of gPKA and analysis of cAMP levels in *G. lamblia* trophozoites.** *A*, at low cell density, anti-gPKA recognizes the intracellular portions of caudal flagella (*CF*), anterior flagella (*AF*), and the basal bodies (*BB*) located between the nuclei. *B*, centrin localization to the posteriolateral flagella. Colocalization of centrin and gPKA was observed to the basal bodies shown in *yellow* and indicated by an *arrow*. *C*, gPKA was associated with basal bodies (*arrow*) and the cytosol, but not the flagella, at high cell densities. *D*, trophozoites that had localized (*L*) staining to caudal flagella and anterior flagella had significantly higher (*) levels of endogenous cAMP, compared with trophozoites that appeared to have diffuse (*d*) staining in the cytosol. Data are represented as mean femtomoles of cAMP/10^5 cells $\pm$ S.D. ($n = 5$).

and altered localization of a protein kinase. Since the flagellar localization was also found after refeeding high density cultures, it is likely a response to growth factors.

Giardia has four pairs of eukaryotic flagella (5) that are responsible for both motility and attachment. Each originates from a basal body between the two nuclei and every pair of flagella traverses part of the cell body and emerges at a specific location. Paraflagellar densities or marginal plates have been observed by electron microscopy, along much of the intracellular portion of all four pairs of flagella, but little is known about the composition or function of the marginal plates (53). Only the extracellular portions of the flagella are covered with plasmalemma.

The ability of trophozoites to alter their flagellar motility in response to external conditions may be critical to their ability to colonize the small intestine where the availability of growth factors is constantly changing. The anterior flagella cross anteriorly from the basal bodies and pass through the cell's ventrolateral flange before exiting the cell body. The ventrolateral flange is the outer margin of the cell body that interdigitates between microvilli of the small intestinal enterocytes (9), along with the ventral adhesive disc in trophozoite attachment. The ventrolateral flagella, stained for centrin, but not for PKA. Both the anterior and ventrolateral flagella are important in forward motion of the trophozoite and continue to beat while the parasite is attached to intestinal enterocytes or to inert substrates. In contrast, the caudal flagella, whose marginal plates also stained for PKA, do not appear to beat during swimming or attachment and have a rigid appearance, very distinct from the helical form of the other flagella (9). The
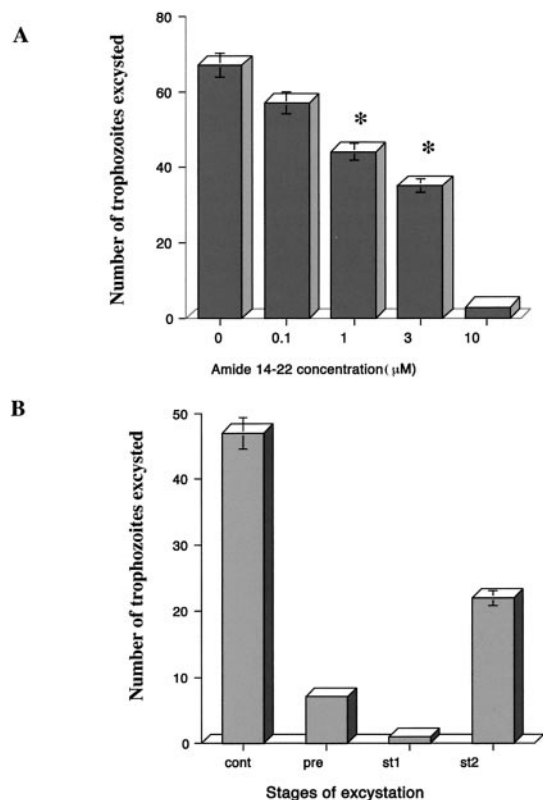
FIG. 6. **Effect of myristoylated PKA inhibitor (amide 14-22) on excystation.** *A*, effect of various concentrations of the inhibitor on excystation. The inhibitor was present at all stages of excystation. Data are represented as mean ± S.D. *, $p < 0.03$ (comparison of untreated with 1 and 3 μM concentrations of the inhibitor). *B*, effect of the inhibitor peptide (14-22) on various stages of excystation. The inhibitor was present at 10 μM only during the stage indicated.

caudal flagella are thought to be associated with dorsal flexion of the "tail" of the cell body that is involved in trophozoite detachment. Since *Giardia* attach to enterocytes, which migrate to the tip of the villus and are then sloughed off, trophozoites must be able to detach, swim, and re-attach to younger host cells to remain in the small intestine. Our finding of association of gPKA with anterior and caudal flagella, whereas centrin associates with the posterior-lateral flagella, may help understand differential flagellar function. Localization of gPKA and centrin to structures responsible for both motility and cell division may link those functions in an ancient eukaryote. These data support a role for PKA and cAMP in regulating giardial attachment and locomotion.

Blocking excystation with the cell permeable PKA inhibitor (amide 14-22) suggests a key role for gPKA in this critical differentiation. The role of PKA appears most critical early in excystation. Cysts are ingested from cold freshwater and are first exposed to the highly acidic gastric fluid (pH 2.0 to pH 4.0), which is needed for the induction of excystation (35) and is modeled by our stage 1 *in vitro*. PKA inactivation prior to or during stage 1 appears to interfere with the induction processes (Fig. 6*B*). Giardial excystation entails a dramatic resumption of flagellar motility and cell division. *In vivo*, excysting cells must regain their motility and attach before they are carried downstream by the flow of intestinal fluid. Therefore, the localization of PKA in flagellar and basal body structures may reflect a role in motility and cytokinesis in excystation as well as in vegetative growth.

Structural analyses of gPKA suggested both a high degree of conservation and possibly significant divergences. Key conserved motifs include the glycine-rich motif, reactive loop, and

Thr-197 residue for autophosphorylation. The most unusual feature of gPKA is a highly stable loop in the activation domain (subdomain VIII) of the enzyme as indicated in the predicted three-dimensional structure (Fig. 2*C*). This loop may interfere with the interaction of gPKA with PKI (6-22 amide) but not with the shorter 14-22 inhibitor or the heptapeptide substrate, kemptide. We hypothesize that gPKA can interact with the shorter inhibitory peptide, but not the longer, possibly because the extra loop in the activation domain of gPKA that could interfere with binding of the larger inhibitor. The catalytic activity of native gPKA should be due to catalytic subunits that have dissociated from the holoenzyme in response to increased cAMP. Exogenous cyclic AMP at a slightly higher concentration than for the mammalian enzyme-activated gPKA activity.

At present, the precise physiological stimuli that affect cAMP levels and PKA activity and localization in *Giardia* are not known. In *Saccharomyces*, the stimuli are very simple; only glucose or cytosolic acidification is known to increase cAMP concentrations. Yeast must respond to transiently favorable growth conditions that allow stationary phase cells to switch to a growth program. Perhaps *Giardia*'s needs are more complex, as its environment changes drastically during excystation. Moreover, within the small intestine, conditions change rapidly according to whether trophozoites are attached to young or senescent enterocytes, or are in the lumen and according to the nutritional status of the host. Our data suggest key roles for PKA in regulating giardial responses to its environment.

REFERENCES

1. Marshall, M. M., Naumovitz, D., Ortega, Y., and Sterling, C. R. (1997) *Clin. Microbiol. Rev.* **10,** 67–85
2. Smith, P. D., Gillin, F. D., Spira, W. M., and Nash, T. E. (1982) *Gastroenterology* **83,** 797–803
3. Adam, R. D. (2000) *J. Parasitol.* **30,** 475–484
4. Bingham, A. K., Jarroll, E. L., Meyer, E. A., and Radulescu, S. (1979) *Exp. Parasitol.* **47,** 284–291
5. Adam, R. D. (1991) *Microbiol. Rev.* **55,** 706–732
6. Rice, E. W., and Schaefer, F. W., III (1981) *J. Clin. Microbiol.* **14,** 709–710
7. Davenport, H. W. (1977) *Physiology of the digestive tract*, Year Book Medical Publishers, Chicago
8. Smith, M. W., Aley, S. B., Sogin, M. L., Gillin, F. D. and Evans, G. (1998) *Mol. Biochem. Parasit.* **95,** 267–280
9. Erlandersen, S. L., and Feely, D. E. (1984) in *Giardia and Giardiasis: Biology, Pathogenesis and Epidemiology* (Erlandsen, S. L., and Meyer, E., eds) pp. 33–63, Plenum Press, New York
10. McKnight, G. S. (1991) *Curr. Opin. Cell Biol.* **3,** 213–217
11. Tramontano, D. Moses, A. C., and Ingbar, S. H. (1988) *Endocrinology* **122,** 133–136
12. Walsh, D. A., Perkins, J. P., and Krebs, E. G. (1968) *J. Biol. Chem.* **243,** 3763–3765
13. Francis, S., and Corbin, J. (1994) *Annu. Rev. Physiol.* **56,** 237–272
14. Kennelly, P. J., and Krebs, E. G. (1991) *J. Biol. Chem.* **266,** 15555–15558
15. Habener, J. F. (1995) in *Endocrinology* (DeGroot, L. J., ed) 3rd Ed., pp. 77–92, W. B. Saunders, Philadelphia
16. Rubin, C. S. (1994) *Biochim. Biophys. Acta* **1224,** 467–479
17. Schillace, R. V., and Scott, J. D. (1999) *J. Clin. Invest.* **103,** 761–765
18. Edwards, A. S., and Scott, J. D. (2000) *Curr. Opin. Cell Biol.* **12,** 217–221
19. Pawson, T., and Scott, J. D. (1997) *Science* **278,** 2075–2080
20. Skalhegg, B. S., and Tasken, K. (1997) *Frontiers Biosci.* **2,** D331–D342
21. Uhler, M. D., Chrivia, J. C., and McKnight, G. S. (1986) *J. Biol. Chem.* **261,** 15360–15363
22. Advani, S. R., Schwarz, M., Showers, M. O., Maurer, R. A., and Hemmings, B. A. (1987) *Eur. J. Biochem.* **167,** 221–0226
23. Shower, M. O., and Maurer, R. A. (1986) *J. Biol. Chem.* **261,** 16288–16291
24. Kalderon, D., and Rubin, G. M. (1988) *Genes Dev.* **2,** 1539–1556
25. Toda, T., Cameron, S., Sass, P., Zoller, M, and Wigler, M. (1987) *Cell* **50,** 277–287
26. Plowman, G. D., Sudarsanam, S., Bingham, J., Whyte, D., and Hunter, T. (1999) *Proc. Natl. Acad. Sci. U. S. A.* **96,** 13603–13610
27. Burki, E. Anjard, C., Scholder, J. C., and Reymond, C. D. (1991) *Gene (Amst.)* **102,** 57–65
28. Simian-Tov, M. M., Aly, R. Shapira, M., and Jaffe, C. L. (1996) *Mol. Biochem. Parasit.* **77,** 201–215
29. Vassella, E., Reuner, B., Yutzy, B., and Boshart, M. (1997) *J. Cell Sci.* **110,** 2661–2671
30. Lasko, P. (1995) *BioEssays* **17,** 105–107
31. Toda, T. Cameron, S., Sass, P., Zoller, M., Scott, J. D., Hurwitz, M. M., Krebs, E. G., and Wigler, M. (1987) *Mol. Cell. Biol.* **7,** 1371–1377

32. Mc Arthur, A. G., Morrison, H. G. Nixon, J. E. J., Passamaneck, N. Q. E., Kim, U., Reich, C. I., Holder, M. E., Hinkle, G., Crocker, M. K., Farr, R., Olsen, G. E., Aley, S. B., Adam, R., Gillin, F. D., and Sogin, M. L. (2000) *FEMS Microbial Lett.* **189,** 271–273
33. Moujou, M., Paintrand, M., Vigues, B., and Bornens, M. (1991) *J. Cell Biol.* **115,** 129–140
34. Keister, D. B. (1983) *Trans. R. Soc. Trop. Med. Hyg.* **77,** 487–488
35. Meng, T. C., Hetsko, M. L., and Gillin, F. D. (1996) *Infect. Immun.* **64,** 2151–2157
36. Chakrabarti, R., McCraken Jr. J. B., Chakrabarti, D., and Souba, W. W. (1995) *Gene* (*Amst.*) **153,** 163–169
37. Peitsch, M. C. (1996) *Biochem. Soc. Trans.* **24,** 274–279
38. Guex, N., and Peitsch, M. C. (1997) *Electrophoresis* **18,** 2714–2723
39. Sambrook, J. Fritsch. E. F., and Maniatis, T. (1989) *Molecular Cloning: A Laboratory Manual*, 2nd Ed., Cold Spring Harbor Laboratory, Cold Spring Harbor, NY
40. Lineweaver, H., and Burk, D. (1934) *J. Am. Chem. Soc.* **56,** 658–666
41. Meng, T.-C., Aley, S. B., Svard, S. G., Smith, M. W., Huang, B., Kim, J., and Gillin, F. D. (1996) *Mol. Biochem. Parasitol.* **79,** 103–108
42. Smith, C. M., Radzio-Andzelm, E., Madhusuda, Akamine, P., and Taylor, S. S. (1999) *Prog. Biophys. Mol. Biol.* **71,** 313–341
43. Sogin, M. L. (1989) *Science* **243,** 75–77
44. Rubin, C. S. (1979) *J. Biol. Chem.* **254,** 12439–12449
45. Cobb, C. E., and Corbin, J. D. (1988) *Methods Enzymol.* **159,** 202–208
46. Kemp, B. E., Benjamini, E., and Krebs, E. G. (1976) *Proc. Natl. Acad. Sci. U. S. A.* **73,** 1038–1042
47. Witczak, O., Skålhegg, B. S., Keryer, G., Bornens, M., Taskén, K., Jahnsen, T., and Ørstavik, S. (1999) *EMBO J.* **18,** 1858–1868
48. Moss, S. B., Turner, R. M., Burkert, K. L., VanScoy, B. H., and Gerton, G. L. (1999) *Biol Reprod.* **61,** 335–342
49. Yang, P., and Sale, W. S. (2000) *J. Biol. Chem.* **275,** 18905–18912
50. Salisbury, J. L. (1995) *Curr. Opin. Cell Biol.* **7,** 39–45
51. Holberton, D. V. (1973) *J. Cell Sci.* **13,** 11–41
52. King, S. (2000) *Biochim. Biophys. Acta* **1496,** 60–75
53. Li, Q., and Bever, C. T., Jr. (1998) *Oncol. Rep.* **5,** 227–233

Possible Roles of Protein Kinase A in Cell Motility and Excystation of the Early Diverging Eukaryote *Giardia lamblia*

Erika S. Abel, Barbara J. Davids, Liza D. Robles, Clarence E. Loflin, Frances D. Gillin and Ratna Chakrabarti